EXPEDITED PUBLICATION

Systemic Exposure to Proteasome Inhibitors Causes a Progressive Model of Parkinson's Disease

Kevin St. P. McNaught, PhD,[1] Daniel P. Perl, MD,[2] Anna-Liisa Brownell, PhD,[3] and C. Warren Olanow, MD[1]

Environmental toxins have been implicated in the etiology of Parkinson's disease. Recent findings of defects in the ubiquitin-proteasome system in hereditary and sporadic forms of the illness suggest that environmental proteasome inhibitors are candidate PD-inducing toxins. Here, we systemically injected six doses of naturally occurring (epoxomicin) or synthetic (Z-lle-Glu(O*t*Bu)-Ala-Leu-al [PSI]) proteasome inhibitors into adult rats over a period of 2 weeks. After a latency of 1 to 2 weeks, animals developed progressive parkinsonism with bradykinesia, rigidity, tremor, and an abnormal posture, which improved with apomorphine treatment. Positron emission tomography demonstrated reduced carbon-11-labeled 2β-carbomethoxy-3β-(4-fluorophenyl)tropane (CFT) binding to dopaminergic nerve terminals in the striatum, indicative of degeneration of the nigrostriatal pathway. Postmortem analyses showed striatal dopamine depletion and dopaminergic cell death with apoptosis and inflammation in the substantia nigra pars compacta. In addition, neurodegeneration occurred in the locus coeruleus, dorsal motor nucleus of the vagus, and the nucleus basalis of Meynert. At neurodegenerative sites, intracytoplasmic, eosinophilic, α-synuclein/ubiquitin–containing, inclusions resembling Lewy bodies were present in some of the remaining neurons. This animal model induced by proteasome inhibitors closely recapitulates key features of PD and may be valuable in studying etiopathogenic mechanisms and putative neuroprotective therapies for the illness.

Ann Neurol 2004;56:149–162

Parkinson's disease (PD) is a slowly progressive neurodegenerative disorder characterized clinically by bradykinesia, rigidity, tremor, gait dysfunction, and postural instability. The primary pathology of PD is degeneration of dopaminergic neurons in the substantia nigra pars compacta (SNc), resulting in loss of the nigrostriatal pathway and a reduction of dopamine levels in the striatum.[1] Neuronal death also occurs in other brain regions, including the locus coeruleus (LC), dorsal motor nucleus of the vagus (DMN), and nucleus basalis of Meynert (NMB),[1] and can be more severe than neuronal death in the SNc.[1,2] At these and other pathological sites, protein-rich structures known as Lewy body inclusions appear in the cytoplasm of some remaining neurons.[1,3]

Recent studies suggest that defects in the capacity of the ubiquitin-proteasome system (UPS) to degrade unwanted proteins may be a common feature in each of the different familial and sporadic forms of PD.[4,5] In rare hereditary forms of PD, mutations in components of the UPS, namely, parkin and ubiquitin C-terminal hydrolase L1, are responsible for development of the illness.[6–8] Also, missense or triplication mutations of the α-synuclein gene are associated with the development of PD.[9–11] It remains unclear as to how alterations in the α-synuclein gene cause neurodegeneration, but it has been shown that misfolded or excess levels of α-synuclein can resist or inhibit the UPS leading to impairment of protein clearance.[12–14]

Most cases of PD occur sporadically and are of unknown cause. In sporadic PD, it is thought that exposure to environmental toxins may be a causative factor, perhaps in individuals rendered susceptible by their genetic profile and/or advancing age.[15] There is also evidence to suggest that, as in familial PD, defects in the UPS could play a role in the pathogenic process occurring in sporadic PD.[5] We and others have demonstrated structural defects and functional impairment of 26/20S

From the Departments of [1]Neurology and [2]Pathology, Neuropathology Division, Mount Sinai School of Medicine, New York, NY; and [3]Department of Radiology, Massachusetts General Hospital/Harvard Medical School, Boston, MA.

Received Apr 22, 2004, and in revised form May 13, 2004. Accepted for publication May 15, 2004.

Published online Jun 21, 2004, in Wiley InterScience (www.interscience.wiley.com). DOI: 10.1002/ana.20186

Address correspondence to Dr McNaught, Department of Neurology, Mount Sinai School of Medicine, Annenberg 14-73, 1 Gustave L. Levy Place, Box 1137, New York, NY 10029.
E-mail: kevin.mcnaught@mssm.edu

proteasomes with the accumulation of undegraded proteins in the SNc in PD.[16–18] Treatment of rat ventral mesencephalic cultures and PC12 cells with proteasome inhibitors leads to degeneration of dopaminergic neurons and the formation of α-synuclein/ubiquitin–containing intracytoplasmic inclusion bodies.[19–21] Furthermore, stereotaxic injection of lactacystin into the SNc, or epoxomicin into the striatum, of rats causes acute degeneration of the nigrostriatal pathway.[22,23] Thus, failure of UPS-mediated proteolysis could be a common factor in the etiopathogenesis of both familial and sporadic PD.

In this study, we examined the possibility that inhibition of proteasomal function and UPS-mediated protein degradation might induce a model of PD. We selected naturally occurring (epoxomicin) and synthetic (PSI, Z-lle-Glu(O*t*Bu)-Ala-Leu-al, a derivative of and closely related to naturally occurring peptide aldehyde inhibitors of the proteasome) inhibitors that can selectively impair the enzyme in an irreversible and a reversible manner, respectively (Fig 1A).[24,25] These toxins, which are lipophilic and can cross the blood–brain barrier, were injected systemically into adult rats. Here, we report that exposure to proteasome inhibitors can induce behavioral, pathological, and neurochemical features of PD.

Materials and Methods

Materials

PSI (Z-lle-Glu(O*t*Bu)-Ala-Leu-al), 3,3′diaminobenzidine hydrochloride (DAB), bovine serum albumin, γ-tubulin antibodies, apomorphine hydrochloride, protease inhibitor cocktail, thioflavin-S, and L-dopa methyl ester were obtained

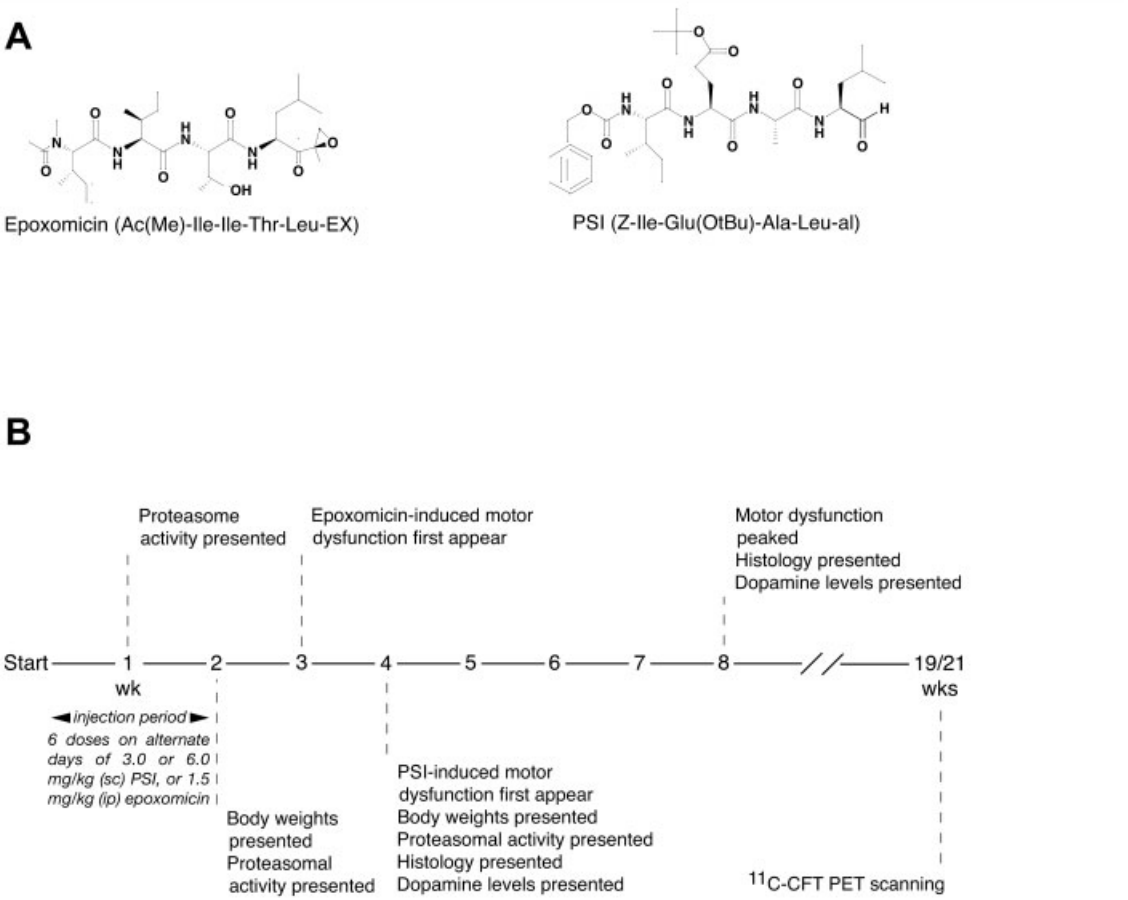

Fig 1. Evaluation of parkinsonian features in adult rats after exposure to proteasome inhibitors. (A) Molecular structures of the irreversible proteasome inhibitor epoxomicin, a peptide epoxyketone naturally produced by Actinomycetes soil bacteria and the reversible proteasome inhibitor PSI, a synthetic peptide aldehyde. (B) Timeline and summary of treatment regimens and analyses. PSI (3.0 or 6.0mg/kg, SC), epoxomicin (1.5mg/kg, IP), or vehicle (70% ethanol or 10% dimethyl sulfoxide) as a control were injected six times into adult Sprague-Dawley rats (approximately 200gm at start) over a period of 2 weeks (Mon, Wed, Fri, Mon, Wed, Fri). At various times after treatments were initiated, a variety of behavioral, imaging, histopathological, and biochemical parameters were assessed. Results presented at each time point normally reflect a sample size of five to seven animals. In the presentation of behavioral changes and body weights, sample sizes are higher (up to 11 per group) because all animals underwent these analyses before they were killed. ^{11}C-CFT = carbon-11-labeled 2β-carbomethoxy-3β [4-flurophenyl]tropane, PET = positron emission tomography.

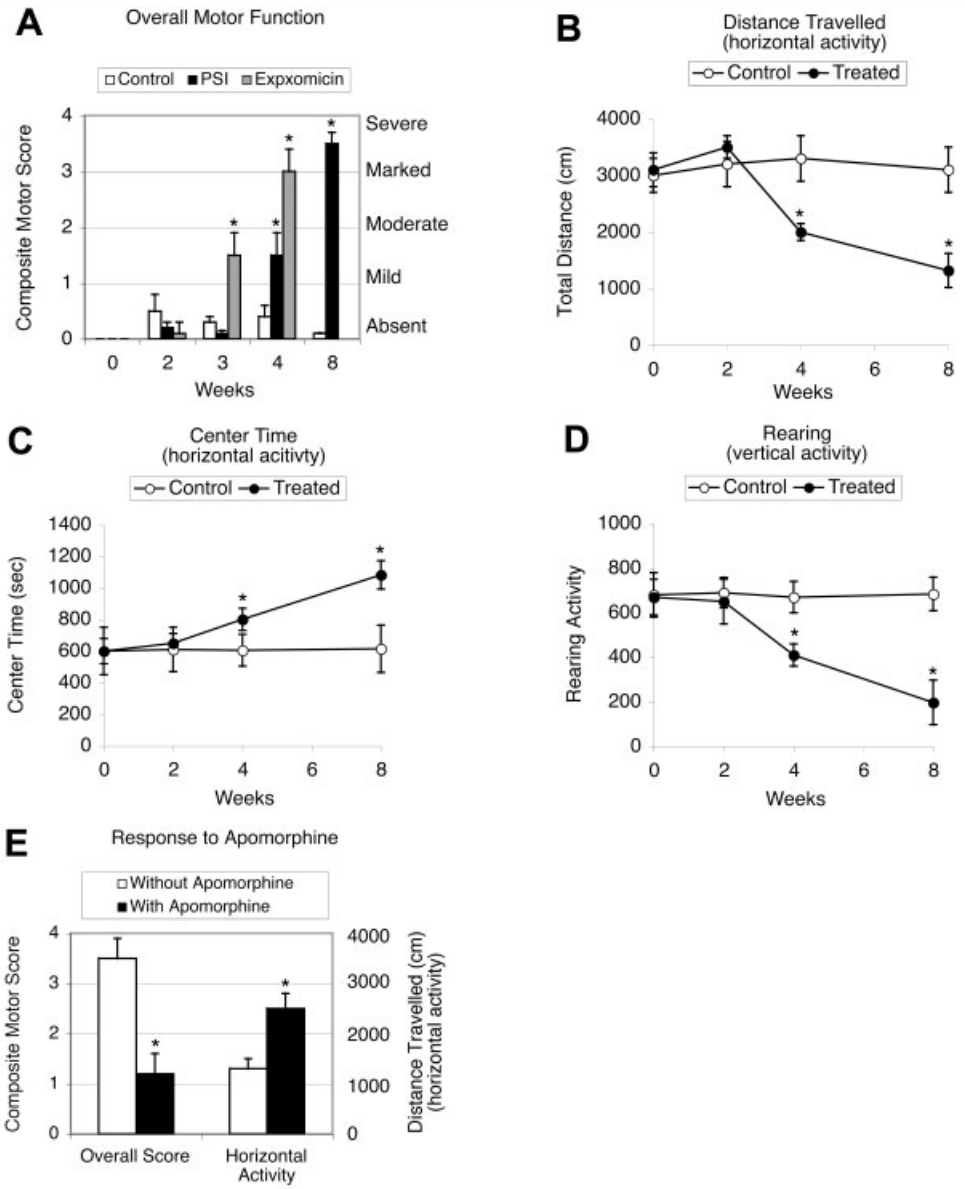

*Fig 2. Behavioral assessment of proteasome-inhibited rats. (A) Before (baseline) and at various times after the initiation of treatments with 3.0mg/kg PSI (n = 11), 1.5mg/kg epoxomicin (n = 6), or vehicle (n = 6–10), rats were assessed for motor activity using a rating scale. Bradykinesia, rigidity, tremor-like limb movements, and abnormal posture were rated in each animal as 0 (absent), 1 (mild), 2 (moderate), 3 (marked), or severe 4 (severe). The composite score represents the mean ± SEM of the different ratings. Note that the epoxomicin group was killed at 4 weeks, and therefore no data are presented at the 8-week time point. Results were analyzed statistically using the Freidman test with Dunnett's post test. *p < 0.01 compared with baseline. (B–D) Rats were treated with PSI as described above. A computerized three-dimensional activity monitoring system, which determines motor activity based on the frequency of interruptions to infrared beams in the* x, y, *and* z *planes, was used to assess motor activity in rats. Results, presented are mean ± SEM (n = 6 per group) and were analyzed statistically using two-way ANOVA with Dunnett's post-test. *p < 0.01 compared with baseline. (E) PSI-treated rats characterized as having severe motor dysfunction were behaviorally assessed before and after (at peak response) administration of apomorphine hydrochloride (1.0mg/kg). Results were analyzed using the Wilcoxon test (motor score) and paired* t*-test (distance traveled) with a sample size of n = 6. (*p < 0.01, comparison of score/activity before and after apomorphine treatment. Composite motor score in this figure includes bradykinesia, rigidity, and abnormal posture but excludes tremor-like limb movements because this behavior did not respond significantly to apomorphine. Note that although animals improved with apomorphine (mean, approximately 72%), motor response was never fully restored to baseline (control) values and suggests that nondopaminergic degeneration might contribute to these behavioral deficits.*

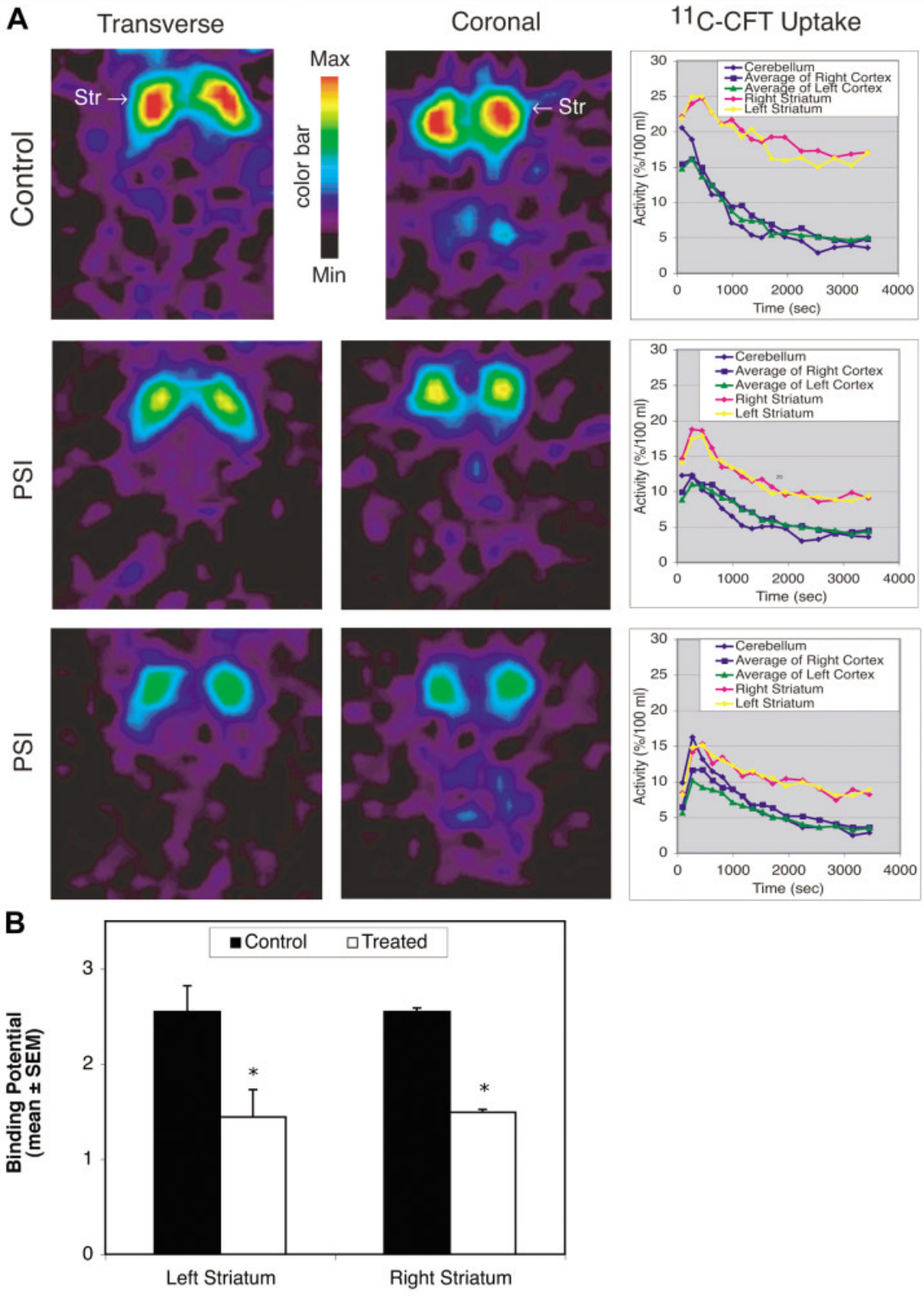

*Fig 3. Positron emission tomography (PET) with ^{11}C-CFT imaging of the striatum in living rats. Several weeks (17–19) after cessation of treatments with 3.0mg/kg PSI or vehicle (controls), rats underwent PET imaging to assess dopaminergic nerve terminal function in the striatum using the specific dopamine transporter ligand carbon-11–labeled 2β-carbomethoxy-3β-(4-fluorophenyl)tropane (^{11}C-CFT). Color bar: maximum (red) and minimum (black) represent a maximum binding ratio of 3.5 and a minimum binding ratio of 0 for ^{11}C-CFT, respectively. The other colors represent intermediate binding levels. (B) A quantification of the images presented in panel A. *$p < 0.01$; $n = 5$ per group, Student's t-test.*

from Sigma-Aldrich Corp (St Louis, MO). Epoxomicin and proteasome substrates were obtained from Calbiochem-Novabiochem Corp (San Diego, CA). Cy5 was obtained from Jackson ImmunoResearch Laboratories (West Grove, PA), and Alexa Fluor 568 and YOYO-1 were obtained from Molecular Probes Inc (Eugene, OR). Antibodies to ubiquitin, α-synuclein, dopamine and cAMP-regulated phosphoprotein 32 (DARP-32), choline acetyltransferase (ChAT), β-synuclein, parkin, and synphilin-1 were obtained from Chemicon International (Temecula, CA). Antibodies (OX-42/CD11b) to activated microglia were obtained from Accurate Chemical and Scientific Corporation (Westbury, NY). Antibodies to tyrosine hydroxylase (TH) were obtained from Pel Freez (Rogers, AR). ^{11}C-CFT (carbon-11–labeled 2β-carbomethoxy-3β-[4-fluorophenyl]tropane) was synthesized by direct methylation of 2β-carbomethoxy-3β-(-4-fluorophenyl)tropane (WIN 35,428; ABX Advanced Biochemical Compounds GmbH, Radeberg, Germany) using ^{11}C-methyliodide as described in detail elsewhere.[26] All other materials were obtained from commercial sources and details are provided in the associated references.

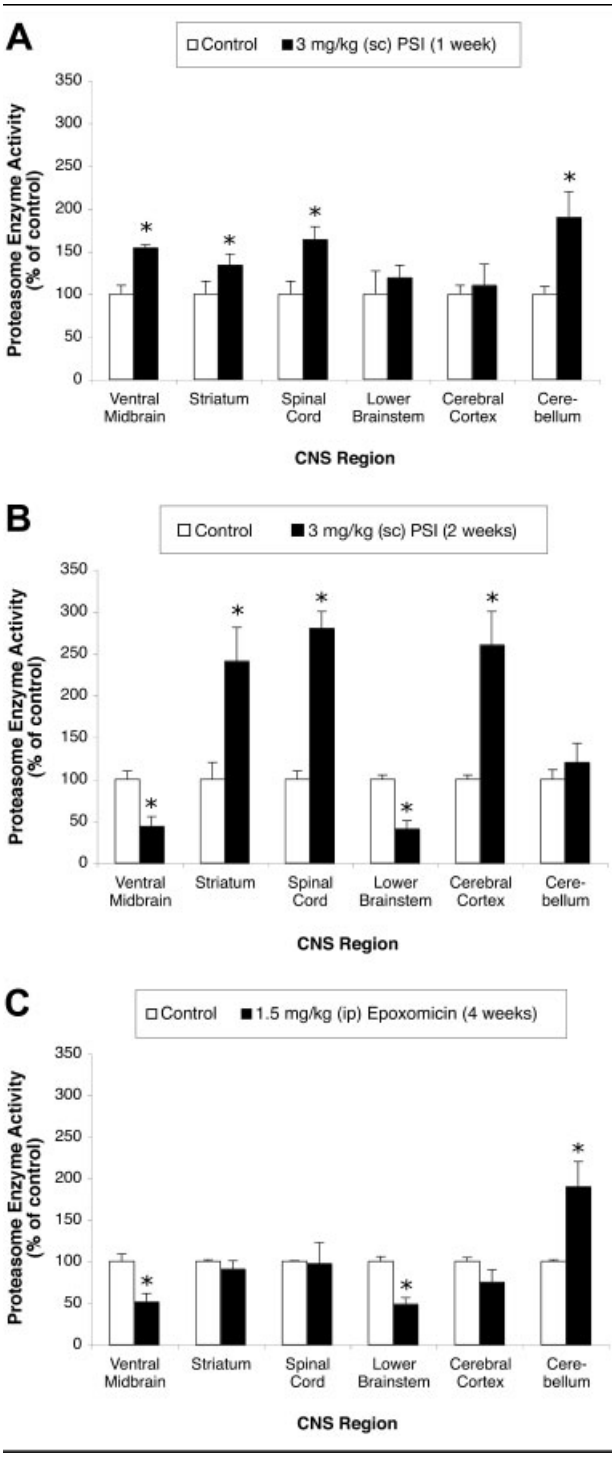

Fig 4. Effects of PSI and epoxomicin on proteasomal function in the rat central nervous system (CNS). The primary chymotrypsin-like activity in CNS tissues from control (unfilled bars) *and PSI/epoxomicin-treated* (filled bars) *rats at 1 week (A), 2 weeks (B) and 4 weeks (C) after the initiation of treatments are presented. Results (mean ± SEM, n = 5 per group) are presented as percentage of control values for the ventral midbrain containing the substantia nigra pars compacta (47.2 ± 3.5 fluorescence units/sec/μg total tissue protein), striatum (817.5 ± 25.2), spinal cord (440.5 ± 35.5), lower brainstem containing the LC and DMN (643.9 ± 132), cerebral cortex (281.7 ± 42.7), and cerebellum (283.6 ± 34.6). Statistical significance was determined using two-tailed Student's* t*-test and Bonferroni correction.* *$p < 0.01$, *treated compared with control.*

Rats and Administration of Proteasome Inhibitors

Sprague-Dawley rats (approximately 200gm) were obtained from Taconic Farms (Germantown, NY). These animals were housed in the Mount Sinai School of Medicine's (MSSM) animal care facility with room temperature/light-dark cycle regulation, and food and water available ad libitum. All experiments involving these animals were approved by the institutional animal care and utilization committee at MSSM.

A total of 70 male Sprague-Dawley rats were used in the following experiments (Fig 1B). Twenty seven (27) rats were injected with 3.0mg/kg (SC) PSI, 3 with 6.0mg/kg (SC) PSI, and 27 with 70% ethanol (SC) as a control. In addition, six animals were injected with 1.5mg/kg (IP) epoxomicin and seven with 10% dimethyl sulfoxide (IP) as a control. In each case, six injections were made over the course of 2 weeks (Mon, Wed, Fri, Mon, Wed, Fri). Rats were examined daily for the first 2 weeks and weekly thereafter for 21 weeks to determine the presence, severity, and progression of motor dysfunction (see Fig 1B).

Behavioral Assessment of Rats for Motor Dysfunction

Rats were videotaped and viewed repeatedly to determine the presence, severity, and progression of motor dysfunctions using a semiquantitative behavioral rating scale which was adapted from a scoring system that is widely used to assess parkinsonian animals.[27] Motor activity and posture were assessed by placing the animals in a large open area where movements and exploration were unrestricted and uninterrupted. Rigidity was assessed by the examiner measuring pas-

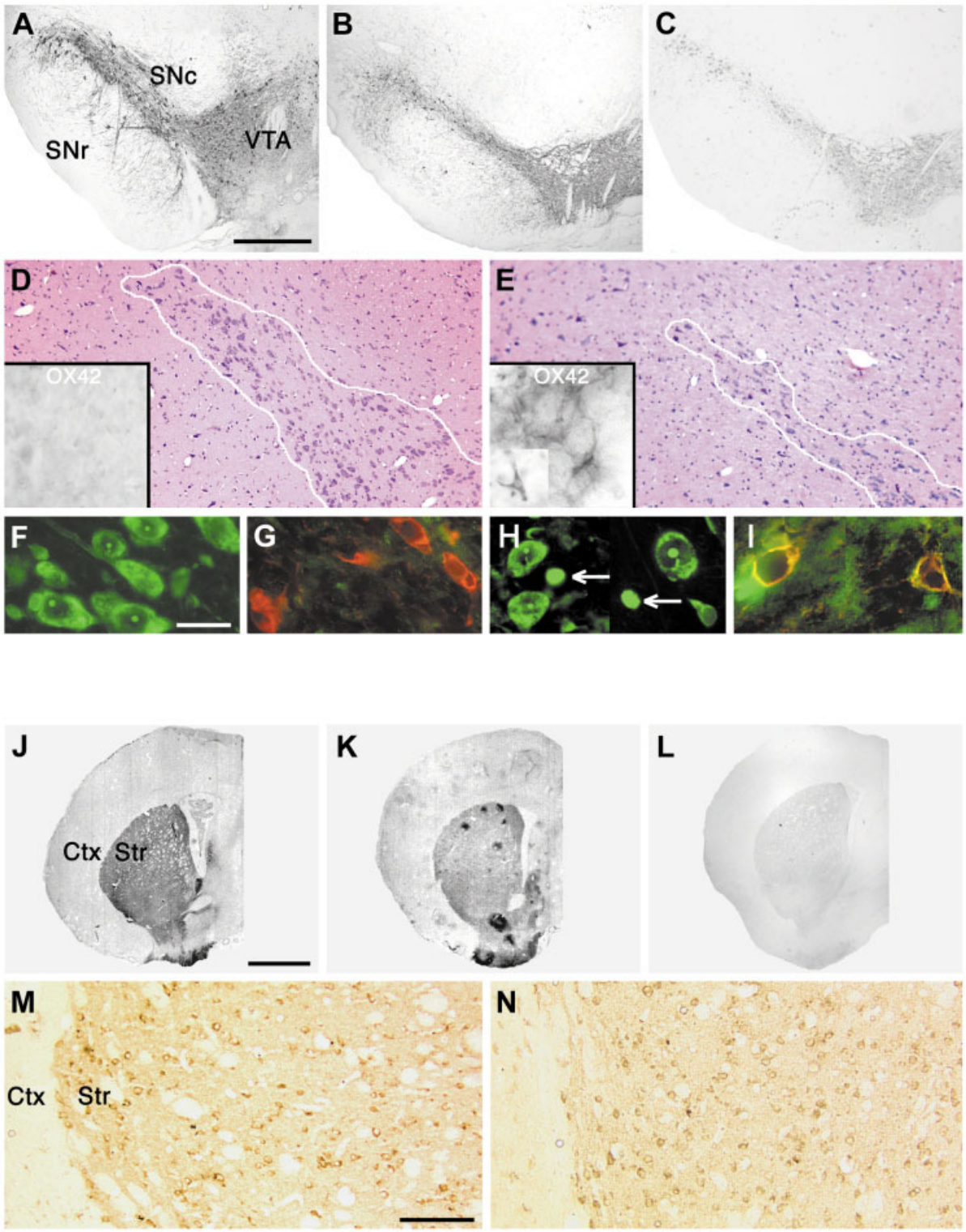

Figure 5

Table. Striatal Levels of Dopamine and Its Metabolites

Treatment Group	Dopamine	DOPAC	HVA
Control	4531 ± 1,798	274 ± 152	1,036 ± 73
Epoxomicin (1.5 mg/kg, IP)	1,282 ± 187[a]	35 ± 4.2[a]	437 ± 61[a]

Striatal levels of dopamine, DOPAC and HVA were determined by high-pressure liquid chromatography HPLC at 2 weeks after the final injection of 1.5 mg/kg (IP) epoxomicin into rats. Data (ng/gm striatal tissue) are presented as mean ± SEM. A sample size of n = 6 for control, and n = 7 for epoxomicin, were used. Results were analyzed statistically using Student's *t* test.

[a] $p < 0.001$.

DOPAC = 3,4-dihydroxyphenylacetic acid; HVA = homovanillic acid.

sive resistance to movement of the limb and tail. Tremor-like limb movements were monitored while these animals were present in their home cage. Motor features were rated as absent (0), mild (1), moderate (2), marked (3), or severe (4). For each animal at each time point, a composite score representing the average of these ratings was calculated.

In addition to the above rating scale, motor function was assessed using a computerized three-dimensional activity monitoring system (AccuScan Instruments, Columbus, OH). This system determines motor activity based on the frequency of interruptions to infrared beams traversing the *x*, *y*, and *z* planes. Total distance (cm) traveled and rearing activity were automatically determined from the interruptions of beams in the horizontal and vertical planes, respectively. Center time was also recorded, reflecting the time that the animals remained in the central location where they initially were placed. All behavioral assessments were conducted blind to treatments by a single investigator (K.M.).

Positron Emission Tomography Imaging

We measured striatal uptake of carbon-11–labeled 2β-carbomethoxy-3β-(4-fluorophenyl)tropane (^{11}C-CFT; 2.5–3.0mCi), a radiolabeled ligand that selectively binds to the dopamine transporter on presynaptic dopaminergic nerve terminals in the striatum,[28] using a microPET P4 small animal four-ring tomograph (Concord Microsystems, Knoxville, TN) as we have described previously.[26,29]

Brain Removal for Histopathological and Biochemical Analyses

When brains were required to conduct only histological studies, rats were killed by terminal anesthesia with 60mg/kg (IP) pentobarbital, followed by transcardial perfusion with 100ml 0.1% heparinized saline (0.9%) and then 200ml of 4% paraformaldehyde (PFA) in phosphate-buffered saline (PBS). Brains were postfixed in 4% PFA for 1 day and cryoprotected in 30% sucrose for 2 days thereafter before being stored in isopentane at −70°C. When brains were required for both biochemical and histopathological studies, animals were decapitated, and the brains were removed and divided midsaggitally. One hemisphere was immediately dissected on ice and then stored at −70°C until required. The other hemisphere was postfixed, cryoprotected, and stored as described above.

Measurement of Proteasomal Function

Brain tissues were homogenized (10% wt/vol) manually and by sonication in ice-cold 50mM Tris-HCl (pH 7.5) containing 1mM K^+EDTA, and protein concentration determined by the Lowry assay with bovine serum albumin as protein standard. Homogenates were kept on ice and used immediately for the fluorometric determination of proteasomal enzymatic activity using a Molecular Devices SpectraMax GeminiXS fluorometric plate reader as described in detail

Fig 5. Progressive degeneration of the nigrostriatal pathway in proteasome-inhibited rats. (A–C) Tyrosine hydroxylase (TH) immunostaining to examine dopaminergic neurons in coronal sections of the midbrain from vehicle (70% ethanol)–treated control rats (A), and animals at 2 (B) and 6 (C) weeks after cessation of treatment with the proteasome inhibitor PSI (3.0mg/kg, sc). Note the reduced TH staining after PSI treatment. SNc = substantia nigra pars compacta; SNr = substantia nigra pars reticulata; VTA = ventral tegmental area. Scale bar = 1mm. (D, E) Hematoxylin and eosin (H&E) staining of adjacent sections to those in panels A to C to visualize the midbrain of rats treated with vehicle (D) or PSI (E) as described above. Note the degeneration of neurons in the SNc (outlined area), but cells immediately below (SNr) and above are spared. These results indicate that reduction in TH immunoreactivity shown in panels A to C is caused by neuronal loss and not downregulation in TH expression. Scale bar (D, F) = 0.5mm. (insets) *Immunostaining using antibodies to OX-42 to visualize microglial activation in PSI-treated rats. Note the appearance of microglial cells in the SNc of rats 6 weeks after cessation of treatment with 3.0mg/kg PSI but not in vehicle-treated control animals. (F–I) Staining of the SNc from control (F, G) and PSI-treated (H, I) rats for nuclear chromatin condensation (F, H) using YOYO-1 or immunofluorescence staining for activated caspase-3 (G, I). In panels G and I, red represents TH-immunoreactive dopaminergic neurons, green is activated caspases-3, and yellow/orange represents the colocalization of TH and activated caspases-3. Scale bar* (insets) *20μm. (J–L) TH immunostaining to visualize nerve terminals of the nigrostriatal pathway in coronal sections of the striatum from control (J) and PSI-treated (K, L) rats at 2 and 6 weeks after cessation of treatment as described above. Scale bar = 2mm. (M, N) DARP-32 (dopamine and cAMP-regulated phosphoprotein-32) to visualize GABAergic neurons in the striatum of vehicle-treated control (M) and PSI-treated rats (N) at 6 weeks after treatment with PSI as described above. Scale bar, 200μm. Ctx = cerebral cortex; Str = striatum.*

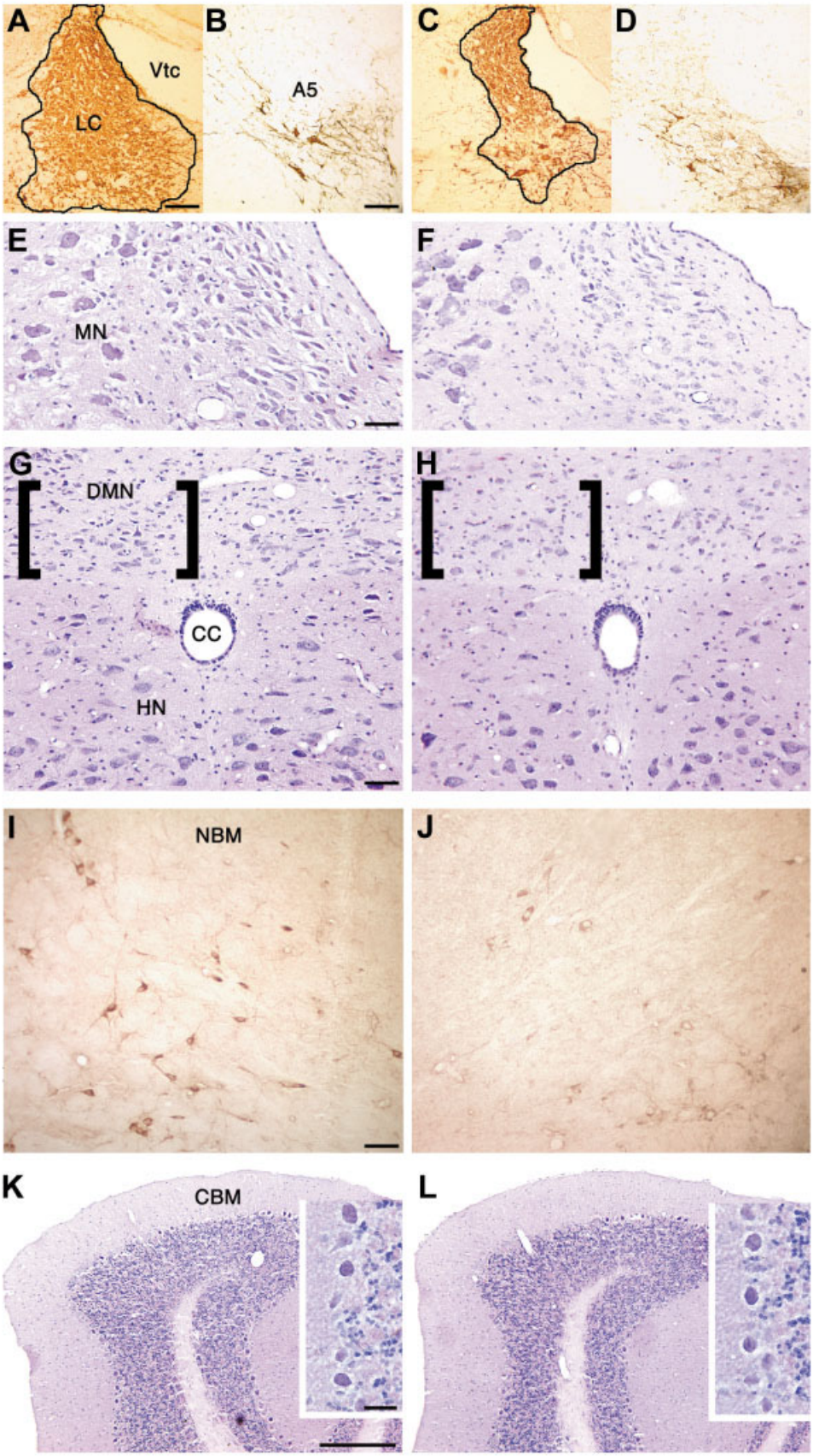

Figure 6

elsewhere.[16,30] Suc-Leu-Leu-Val-Try-AMC, Boc-Leu-Arg-Arg-AMC, and Z-Leu-Leu-Glu-AMC were used as substrates to measure the chymotrypsin-like, trypsin-like, and peptidyl glutamylpeptide hydrolytic proteolytic activities, respectively. Proteasomal enzymatic rates (initial linear portion of reaction sensitive to 10μm epoxomicin/lactacystin) are expressed as fluorescence units/sec/μg brain tissue protein.

Histopathological Assessment of Neurodegeneration

Coronal sections (20μm) were cut through the entire brain using a Leica CM3050 cryostat and mounted on glass slides. Sections were either stained using a Vector ABC immunostaining procedure with DAB chromogen and hematoxylin counterstain; or a double immunofluorescence method with Cy5/Alexa Fluor 568-linked secondary antibodies; or a standard hematoxylin and eosin (H&E) protocol.[17] The number of neuronal cell bodies in specific brain areas were counted manually in every seventh section extending rostrocaudally as we described previously.[31] Cell counts were performed blind for treatment groups receiving vehicle only, PSI, or epoxomicin.

Quantification of Striatal Levels of Dopamine and its Metabolites

Striata were homogenized (10% wt/vol) by sonication in ice-cold 0.4M perchloric acid with 3,4-dihydroxybenzylamine (DHBA) as internal standard. Homogenates were centrifuged at 25,000*g* for 10 minutes at 4°C and supernatants were collected. The levels dopamine (DA), 3,4-dihydroxyphenylacetic acid (DOPAC), and homovanillic acid (HVA) were determined by high-pressure liquid chromatography (HPLC) with electrochemical detection as previously described.[32] Concentrations of analyte were determined automatically using the peak height ratio method and expressed as nanograms per grams striatal tissue based on original wet weight.

Results

General Effects of Proteasome Inhibitors

Rats did not exhibit evidence of systemic toxicity or paralysis and none died. All animals retained the ability to feed and groom. PSI, at either 3.0mg/kg or 6.0mg/kg, had no effect on weight gain compared with controls. At 2 and 4 weeks after initiation of treatment, mean body weights were, respectively, 291.8 ± 5.6gm and 381 ± 10gm for controls (n = 8) compared with 290.8 ± 5.1 and 386 ± 9.4 for PSI-treated animals (n = 8). The mean body weight of epoxomicin-treated rats at 2 weeks was 17.7% lower than vehicle-treated controls (238.4 ± 11.4gm and 289.7 ± 6.2g; n = 6 and 7, $p = 0.006$, Student's *t* test), but there was no significant difference between groups at 4 weeks (334.9 ± 13.7gm and 361 ± 20.6; n = 6 and 7, $p = 0.19$, Student's *t*-test). Neither PSI nor epoxomicin had any later effect on body weight.

Development of Progressive Parkinsonism

Behavioral analyses were performed by an observer blinded to treatment groups (K.M.). No behavioral changes were observed at any time in any of the control animals. At approximately 1 week after the last dose of epoxomicin and 2 weeks after the last administration of either dose of PSI, all treated animals developed mild motor slowing or bradykinesia (Fig 2A–D). During the next 4 weeks, motor dysfunction gradually progressed until all 27 PSI- and all 6 epoximicin-treated animals demonstrated severe bradykinesia accompanied by the presence of moderate-severe rigidity and abnormal posture (see Fig 2A–D). Rats also displayed intermittent, brief episodes (up to 3 seconds), of tremor-like movements in one or both forelimbs when rearing on hindlimbs. However, it is not possible to state with certainty whether this was a resting or postural tremor. Administration of apomorphine hydrochloride (1.0mg/kg, SC) or L-dopa methyl ester (50mg/kg, IP) to PSI-treated rats resulted in an improvement of motor activities, most notably in bradykinesia, rigidity, and posture (see Fig 2E). No spontaneous behavioral recovery was observed during the 21 weeks of continued observation.

Fig 6. Proteasome inhibitors cause selective neurodegeneration in rats. (A–D) Tyrosine hydroxylase (TH) immunostaining to examine noradrenergic neurons in the locus coeruleus (LC) and A5 nucleus of vehicle (70% ethanol)–treated control rats (A, B) and animals 6 weeks (C, D) after the cessation of treatment with the proteasome inhibitor PSI (3.0mg/kg, sc). Vtc = ventricle. Similar results were obtained using dopamine β-hydroxylase immunostaining (not shown). Scale bar = 100μm. (E, F) Hematoxylin and eosin (H&E) staining of adjacent sections to those in panels A to D to visualize the LC and surrounding brainstem areas from control rats (E) and rats treated with PSI (F) as described above. Note the loss of neurons in the LC but relative sparing of neighboring cells in the mesencephalic nucleus (MN) of proteasome-inhibited rats. These results with H&E also demonstrate that reductions in TH immunoreactivity shown in panels A to D are caused by neuronal loss and not downregulation in TH expression. Scale bar = 100μm. (G, H) H&E staining of lower brainstem areas shows neurons in the dorsal motor nuclei of the vagus (DMN) and hypoglossal nuclei (HN) of rats treated with vehicle (G) and PSI (H) as described above. Note the loss of neurons in the DMN on both sides as indicated by brackets. CC = central canal. Scale bar = 100μm. (I, J) Choline acetyltransferase (ChAT) immunostaining to visualize cholinergic neurons (brown DAB chromogen) in the nucleus basalis of Meynert (NBM) of vehicle-treated control rats (I), and animals 6 weeks (J) after the cessation of treatment with PSI. Scale bar = 100μm. (K, L) H&E staining of sections from the cerebellum of vehicle (70% ethanol)–treated control rats (K) and animals 6 weeks (L) after the cessation of treatment with the proteasome inhibitor PSI. Insets are higher magnifications of the Purkinje cell layer. Scale bar (K, L) = 0.5mm. NBM = nucleus basalis of Meynert. CMB = cerebellum, Vtc = ventricle.

Striatal Uptake of ^{11}C-CFT Using Positron Emission Tomography Analysis

Positron emission tomography (PET) imaging with ^{11}C-CFT was performed at 17 to 19 weeks after the final injection of 3mg/kg PSI (see Fig 3A). Compared with animals treated with vehicle (control), rats treated with PSI showed bilateral reductions in striatal ^{11}C-CFT binding (left, 43.4 ± 1.5%; right, 41.5 ± 1.3%; see Fig 3B).

Postmortem Analyses

Rats were killed at 2 and 6 weeks after cessation of treatment with proteasome inhibitors or vehicle. Brains were removed and processed for biochemical and histopathological evaluations. The anatomic and cellular specificity of neurodegeneration induced by PSI and epoxomicin were similar, although the latter compound produced behavioral changes 1 week earlier, and PSI at 6.0mg/kg was only slightly more neurotoxic than when administered at 3mg/kg (assessed at 6 weeks after final administration). The description that follows refers specifically to animals treated with PSI at 3.0mg/kg unless otherwise stated.

ALTERED PROTEASOMAL FUNCTION IN THE CENTRAL NERVOUS SYSTEM. Proteasomal enzymatic activities were determined in several central nervous system (CNS) regions at different time points after commencing treatment with vehicle, PSI, or epoxomicin (Fig 1B). In control rats, proteasomal function varied among the different CNS regions as previously reported, with the lowest activity found in the ventral midbrain which contains the SNc.[16,33] One week after initiating treatment with PSI, there was an increase in proteasomal activity compared with controls in most CNS regions examined, although only some changes were statistically significant ($p < 0.01$; see Fig 4A). This finding suggests an early upregulation in the transcription, translation, and/or activity of proteasomal components in response to PSI treatment, a phenomenon that has been reported in other model systems.[34] After 2 weeks, proteasomal function in the cerebral cortex, striatum, cerebellum, and spinal cord remained elevated, but there was a notable reduction in proteasomal function in the ventral midbrain (56.4 ± 11.6%, $p < 0.01$) and lower brainstem 59.4 ± 9.8 %, $p < 0.01$) compared with controls (see Fig 4B). Similar results were obtained with epoxomicin, in which 4 weeks after treatment was initiated, proteasomal function in the cerebellum was elevated and activities in the spinal cord and striatum were unchanged, but proteasomal function was reduced by 48.5 ± 7.9% ($p < 0.01$) in the ventral midbrain and by 51.4 ± 9.8% ($p < 0.01$) in the lower brainstem (see Fig 4C). This compensatory upregulation in proteasomal activity in various brain regions such as the striatum and cerebral cortex, but or reduced activity in the SNc, has been shown to occur in the brain of PD patients.[16] These findings suggest that neurons in the ventral midbrain and possibly the lower brainstem have a relatively poor ability to mount or maintain compensatory proteolytic mechanisms, which could contribute to their susceptibility to degenerate. There were no significant differences in the enzymatic activities of calpain, and lysosomal cathepsins A and B, in the various CNS regions of PSI-/epoxomicin-treated rats compared with controls (data not shown). This finding demonstrates that PSI and epoxomicin inhibit the proteasome in a selective manner under the experimental conditions used in this study.

DEGENERATION OF THE NIGROSTRIATAL PATHWAY. Immunostaining for TH-containing dopaminergic neurons in the midbrain of vehicle-treated control rats showed abundant cell bodies and processes in the SNc and ventral tegmental area (VTA; Fig 5A). In contrast, there was a progressive decline in the number of TH-immunoreactive cell bodies and processes in the SNc of proteasome-inhibited animals (see Fig 5B, C). Interestingly, the lateral portion of the SNc was more affected than the medial region, and VTA neurons were relatively spared (see Fig 5B, C). Quantification of the extent of neurodegeneration in the SNc of proteasome-inhibited rats showed that TH-positive cell loss was 53% ± 7.2% ($p < 0.01$, Student's t-test, n = 6 per group) at 2 weeks and 72.3 ± 4.2% ($p < 0.01$, n = 6 per group) at 6 weeks. Two weeks after the final administration of 1.5mg/kg epoxomicin, the extent of TH-positive cell loss in the SNc compared with controls was 62% ± 3.2% ($p < 0.01$, Student's t test, n = 6 and 7 for epoxomicin and control). Staining of adjacent sections with hematoxylin and eosin (H&E) demonstrated a lack of neurodegeneration in regions immediately ventral (substantia nigra pars reticulata [SNr]) and dorsal to the SNc (see outlined area Fig 5D, E).

We immunostained brain sections with antibodies to OX-42 (CD11b), a marker of activated microglia,[35] to determine whether an inflammatory reaction occurs in the SNc of proteasome-inhibited rats. In control animals, there was little immunostaining in the SNc, but in rats treated with PSI, there was a marked increase in OX-42 immunoreactivity with the appearance of numerous microglial cells (see Fig 5D, E, insets).

In the SNc of proteasome-inhibited animals but not in controls, YOYO-1 staining demonstrated nuclear chromatin condensation (Fig. 5F,H) and there was increased immunoreactivity for activated caspase-3 (Fig 5. G,I). These findings indicate that cell death occurred, at least in part, by apoptosis.[36]

Consistent with the loss of dopaminergic neurons in the SNc, there was a progressive and uniform decline in the density of TH-immunoreactive nerve terminals in the striatum of proteasome-inhibited rats in comparison with controls (see Fig 5J–L). This was associated with a marked depletion in the levels of dopamine and its metabolites in the striatum of PSI- and epoxomicin-treated rats (Table). DARP-32 (dopamine and cAMP-regulated phosphoprotein-32) (see Fig 5M, N) and choline acetyltransferase staining (data not shown), specific markers of GABAergic and cholinergic neurons, respectively, were not affected in proteasome-inhibited compared with control rats.

NEURODEGENERATION IN THE LOCUS COERULEUS, DORSAL MOTOR NUCLEUS OF THE VAGUS, AND NUCLEUS BASALIS OF MEYNERT In addition to cell loss in the SNc, there was marked cellular degeneration in the LC, DMN, and NBM in animals treated with the proteasome inhibitors (Fig 6). Quantification of cell loss in these regions at 6 weeks after PSI administration showed that, in comparison with vehicle-treated controls, there was a 64.3 ± 5.2% ($p < 0.01$, Student's t-test, n = 6 and 5 for PSI and control), 58.1 ± 4.2% ($p < 0.01$), and 72.4 ± 14.2% ($p < 0.01$) loss of cells in the LC (TH/dopamine β-hydroxylase-positive), DMN (H&E stained) and NBM (ChAT–positive), respectively. Interestingly, although there was prominent degeneration of TH-immunoreactive noradrenergic neurons in the LC (see Fig 6A, C), noradrenergic neurons were unaffected in the more ventrally located A5 nucleus (see Fig 6B, D). Similarly, H&E staining showed relative sparing of cells in the mesencephalic nucleus, which is in the immediate vicinity of the LC (see Fig 6E, F), and of cells in the hypoglossal nucleus, which is proximate to the DMN (see Fig 6G, H). We found no evidence of cell loss in the cerebellum (see Fig 6K, L), or in selected regions of the cerebral cortex that were examined (not shown) in proteasome-inhibited rats when compared with controls.

FORMATION OF INCLUSION BODIES In rats treated with proteasome inhibitors, but not in controls, intracellular protein accumulation and intracytoplasmic inclusions of varying sizes (6–10μm) and numbers were seen in neurons of the SNc, LC, and DMN (Fig 7). With

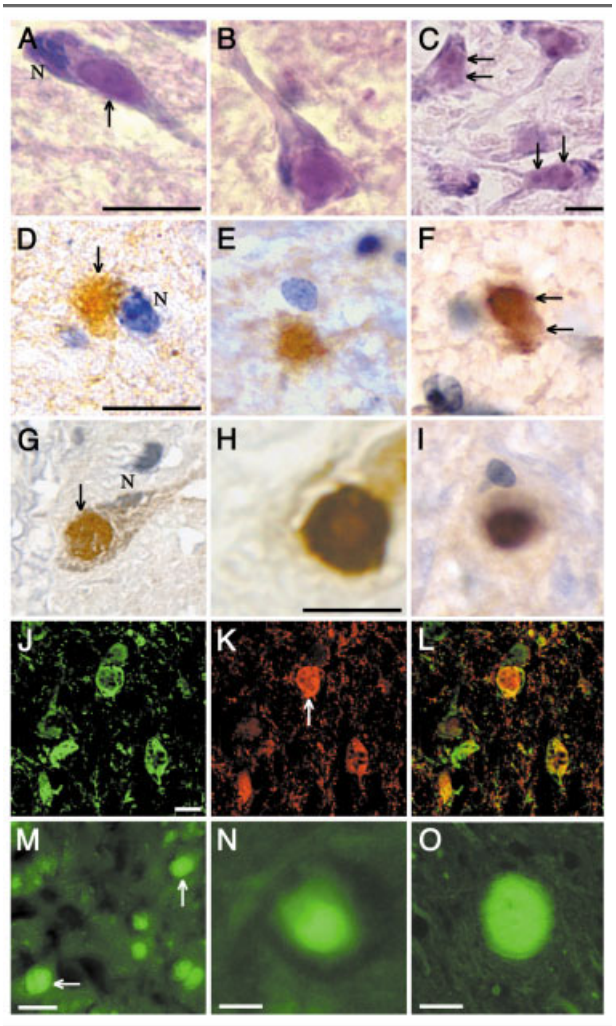

Fig 7. Formation of Lewy body–like inclusions in proteasome-inhibited rats. (A–C) H&E staining of the substantia nigra pars compacta (SNc) (A, B) and locus coeruleus (LC) (C) sections from rats 6 weeks after the cessation of treatment with PSI (A, C; 3.0mg/kg) or 2 weeks after cessation of treatment with epoxomicin (B; 1.5mg/kg). Note the presence of a pink eosinophilic inclusion body (arrows) *in cells of the SNc (A, B) and two inclusions in two cells of the LC (C). Blue structures (N) are hematoxylin-stained nuclei. Scale bar = 10μm. (D–I) Immunostaining with a DAB chromogen (brown) shows the presence of α-synuclein (D, E), synphilin-1 (F), ubiquitin (G, H), and γ-tubulin (I)–immunoreactive inclusion bodies* (arrows) *in the SNc (D–I, except E) and dorsal motor nucleus of the vagus (E) from rats treated with PSI. Blue circular structures are hematoxylin-stained nuclei (N). Note the presence of two adjacent synphilin-1–immunoreactive inclusions (F,* arrows*) in a cell in the SNc. Scale bar (D–I, except H) = 10μm. Scale bar (H) = 5μm. (J–L) Using a fluorescence-based double-immunostaining technique to label TH (J) and α-synuclein (K) proteins in the same SNc sections and cells, α-synuclein-immunoreactive inclusion bodies can be seen within dopaminergic neurons (L, overlay of J and K). Similar double-immunostaining techniques also showed colocalization of TH with ubiquitin, synphilin-1, γ-tubulin, and parkin in the SNc and LC (not shown). Scale bar = 10μm. (M–O) Demonstration that the inclusions formed in the SNc of proteasome-inhibited rats are thioflavin-S reactive. M inclusion bodies in the SNc of PSI-treated rats. N, inclusion bodies in the SNc of epoxomicin-treated rats. (O) A control for thioflavin-S reactivity shows a positively stained Lewy body in the SNc of a patient with PD. Scale bars = 10μm (M) and 2.5μm (N, O).*

H&E stains, these structures exhibited a densely stained central core surrounded by a lighter stained periphery (see Fig 7A–C). These inclusions also displayed prominent immunoreactivity for α-synuclein, synphilin-1, ubiquitin, γ-tubulin and parkin (see Fig 7D–L), but not for β-synuclein (not shown). The intracellular inclusion bodies formed in proteasome-inhibited rats demonstrated reactivity to thioflavin-S (see Fig 7M, N), which is a fluorescent amyloid dye that detects fibrillar proteins (β-pleated sheets) such as filamentous α-synuclein in Lewy bodies in PD patients[37] (see Fig 7O).

Discussion

We show that systemic exposure of rats to naturally occurring and synthetic inhibitors of the proteasome induces a model of PD. After a latency of 1–2 weeks, treated animals developed a gradually progressive, L-dopa/apomorphine-responsive, parkinsonian syndrome with a decrease in striatal ^{11}C-CFT binding on PET. Pathologically, there was neurodegeneration in the SNc, as well as in the LC, DMN, and NBM, a pattern of neuronal loss similar to what is found in PD. Furthermore, neurodegeneration was accompanied by intracytoplasmic Lewy body–like inclusions that stained positively for α-synuclein, ubiquitin, and other proteins. Thus, proteasome inhibitors can induce a parkinsonian syndrome in rats that closely recapitulates many of the features of PD.

The model of PD induced by proteasome inhibitors has several advantages over previously described models of the illness caused by toxins. The MPTP model of PD is acute and nonprogressive, pathology is confined to the nigrostriatal system, and the model is not associated with the formation of inclusion bodies.[38] Rotenone induces degeneration of the SNc with inclusion body formation in rats,[39] but this compound also causes more widespread degeneration with the involvement of striatal and cerebellar neurons, a pattern that is not typical of what is seen in PD.[40,41] Furthermore, rotenone induces systemic toxicity such that 35 to 50% of animals die.[39–42] In contrast, the model of PD induced by proteasome inhibitors has a delayed onset, is associated with a progressive parkinsonian syndrome in all exposed animals, and does not cause paralysis, generalized toxicity, or death. Indeed, the slow progression of the model over several weeks after treatment is stopped suggests that the neurodegenerative process may be self-sustaining once initiated. Second, neurodegeneration induced by proteasome inhibitors is not confined to the nigrostriatal system but includes other structures such as the LC, DMN, and NBM that are also involved in PD.[1] Finally, we note the formation of Lewy body–like inclusions in neurons of the SNc as well as in the LC and DMN of proteasome-inhibited rats as seen in PD. Thus, the rat model of PD based on proteasomal inhibition that we now describe more closely recapitulates features of the illness in humans than other models.

Based on the findings in this study, it is interesting to speculate on the possibility that exposure to proteasome inhibitors could underlie some cases of PD. Proteasome inhibitors are widely distributed in the environment,[25] being produced by bacteria (eg, actinomycetes which infect the below ground portion of crops),[43,44] fungi (eg, *Apiospora montagne* which infest wheat/flour),[45] plants,[46–48] and possibly the chemical industry.[25] Indeed, lactacystin and epoxomicin, which are naturally produced by actinomycetes (*Streptomyces*), are found globally in soil and aquatic habitats of garden and farmland.[49,50] These microbes can also can infect root vegetables and potatoes causing "scab" formation.[49,50] It is thus noteworthy that potent proteasome inhibitors are found in rural areas and in well water, both of which have been shown to be associated with an increased risk of developing PD in epidemiological studies.[51] In addition, structural analogs and the active pharmacophore of natural and synthetic compounds known to potently inhibit the proteasome, such as PSI, are also present in the environment.[25] Thus, exposure to certain microorganisms, or ingestion of foods and water containing proteasome inhibitors, may represent a means by which these compounds could enter the human body.

In conclusion, we show that naturally occurring and synthetic inhibitors of proteasomal function can induce a progressive neurodegenerative disorder in rats that closely recapitulates the features of PD. These studies raise the possibility that similar toxins in the environment could cause or contribute to the development of the illness in susceptible individuals. In addition, this progressive animal model of PD could provide new insights into UPS-related and other mechanisms involved in the neurodegenerative process and may be useful in developing and testing neuroprotective therapies.

This work was supported by the Bendheim Parkinson's Disease Center (K.M., C.W.O.), the Bachmann-Strauss Dystonia and Parkinson Foundation Inc. (K.M., C.W.O.), the Shapiro Foundation (K.M., C.W.O.), and the NIH (National Institute of Neurological Disorders and Stroke, 1 RO1 NS045999-01, K.M., C.W.O.).

We thank T. M. C. Jackson, T.-A. Jengelley, R. JnoBaptiste, A. Kapustin, and G. D. Bouyer for technical assistance.

References

1. Braak H, Tredici KD, Rub U, et al. Staging of brain pathology related to sporadic Parkinson's disease. Neurobiol Aging 2003; 24:197–211.
2. Zarow C, Lyness SA, Mortimer JA, Chui HC. Neuronal loss is greater in the locus coeruleus than nucleus basalis and substantia nigra in Alzheimer and Parkinson diseases. Arch Neurol 2003;60:337–341.

3. Forno LS. Neuropathology of Parkinson's disease. J Neuropathol Exp Neurol 1996;55:259–272.
4. Dawson TM, Dawson VL. Molecular pathways of neurodegeneration in Parkinson's disease. Science 2003;302:819–822.
5. McNaught KS, Olanow CW. Proteolytic stress: a unifying concept in the etiopathogenesis of familial and sporadic Parkinson's disease. Ann Neurol 2003;53(suppl 1):S73–S86.
6. Kitada T, Asakawa S, Hattori N, et al. Mutations in the parkin gene cause autosomal recessive juvenile parkinsonism. Nature 1998;392:605–608.
7. Shimura H, Schlossmacher MG, Hattori N, et al. Ubiquitination of a new form of α-synuclein by parkin from human brain: implications for Parkinson's disease. Science 2001;293: 263–269.
8. Leroy E, Boyer R, Auburger G, et al. The ubiquitin pathway in Parkinson's disease. Nature 1998;395:451–452.
9. Polymeropoulos MH, Lavedan C, Leroy E, et al. Mutation in the alpha-synuclein gene identified in families with Parkinson's disease. Science 1997;276:2045–2047.
10. Kruger R, Kuhn W, Muller T, et al. Ala30Pro mutation in the gene encoding alpha-synuclein in Parkinson's disease. Nat Genet 1998;18:106–108.
11. Singleton AB, Farrer M, Johnson J, et al. alpha-Synuclein locus triplication causes Parkinson's disease. Science 2003;302:841.
12. Snyder H, Mensah K, Theisler C, et al. Aggregated and monomeric alpha-synuclein bind to the S6′ proteasomal protein and inhibit proteasomal function. J Biol Chem 2003;278: 11753–11759.
13. Tanaka Y, Engelender S, Igarashi S, et al. Inducible expression of mutant alpha-synuclein decreases proteasome activity and increases sensitivity to mitochondria-dependent apoptosis. Hum Mol Genet 2001;10:919–926.
14. Stefanis L, Larsen KE, Rideout HJ, et al. Expression of A53T mutant but not wild-type alpha-synuclein in PC12 cells induces alterations of the ubiquitin-dependent degradation system, loss of dopamine release, and autophagic cell death. J Neurosci 2001;21:9549–9560.
15. Tanner CM. Is the cause of Parkinson's disease environmental or hereditary? Evidence from twin studies. Adv Neurol 2003; 91:133–142.
16. McNaught KS, Belizaire R, Isacson O, et al. Altered proteasomal function in sporadic Parkinson's disease. Exp Neurol 2003; 179:38–45.
17. McNaught KS, Shashidharan P, Perl DP, et al. Aggresome-related biogenesis of Lewy bodies. Eur J Neurosci 2002;16: 2136–2148.
18. Tofaris GK, Razzzaq A, Ghetti B, et al. Ubiquitination of alpha-synuclein in Lewy bodies is a pathological event not associated with impairment of proteasome function. J Biol Chem 2003;278:44405–44411.
19. McNaught KSP, Mytilineou C, JnoBaptiste R, et al. Impairment of the ubiquitin-proteasome system causes dopaminergic cell death and inclusion body formation in ventral mesencephalic cultures. J Neurochem 2002;81:301–306.
20. Petrucelli L, O'Farrell C, Lockhart PJ, et al. Parkin protects against the toxicity associated with mutant alpha-synuclein: proteasome dysfunction selectively affects catecholaminergic neurons. Neuron 2002;36:1007–1019.
21. Rideout HJ, Larsen KE, Sulzer D, Stefanis L. Proteasomal inhibition leads to formation of ubiquitin/alpha-synuclein-immunoreactive inclusions in PC12 cells. J Neurochem 2001; 78:899–908.
22. McNaught KSP, Bjorklund LM, Belizaire R, et al. Proteasome inhibition causes nigral degeneration with inclusion bodies in rats. Neuroreport 2002;13,:1437–1441.
23. Fornai F, Lenzi P, Gesi M, et al. Fine structure and biochemical mechanisms underlying nigrostriatal inclusions and cell death after proteasome inhibition. J Neurosci 2003;23: 8955–8966.
24. Kozlowski L, Stoklosa T, Omura S, et al. Lactacystin inhibits cathepsin A activity in melanoma cell lines. Tumour Biol 2001; 22:211–215.
25. Kisselev AF, Goldberg AL. Proteasome inhibitors: from research tools to drug candidates. Chem Biol 2001;8:739–758.
26. Brownell AL, Elmaleh DR, Meltzer PC, et al. Cocaine congeners as PET imaging probes for dopamine terminals. J Nucl Med 1996;37:1186–1192.
27. Imbert C, Bezard E, Guitraud S, et al. Comparison of eight clinical rating scales used for the assessment of MPTP-induced parkinsonism in the Macaque monkey. J Neurosci Methods 2000;96:71–76.
28. Rinne JO, Ruottinen H, Bergman J, et al. Usefulness of a dopamine transporter PET ligand [(18)F]beta-CFT in assessing disability in Parkinson's disease. J Neurol Neurosurg Psychiatry 1999;67:737–741.
29. Brownell AL, Livni E, Galpern W, Isacson O. In vivo PET imaging in rat of dopamine terminals reveals functional neural transplants. Ann Neurol 1998;43:387–390.
30. Craiu A, Gaczynska M, Akopian T, et al. Lactacystin and clasto-lactacystin beta-lactone modify multiple proteasome beta-subunits and inhibit intracellular protein degradation and major histocompatibility complex class I antigen presentation. J Biol Chem 1997;272:13437–13445.
31. Bjorklund LM, Sanchez-Pernaute R, Chung S, et al. Embryonic stem cells develop into functional dopaminergic neurons after transplantation in a Parkinson rat model. Proc Natl Acad Sci USA 2002;99:2344–2349.
32. Kalir HH, Mytilineou C. Ascorbic acid in mesencephalic cultures: effects on dopaminergic neuron development. J Neurochem 1991;57:458–464.
33. Keck S, Nitsch R, Grune T, Ullrich O. Proteasome inhibition by paired helical filament-tau in brains of patients with Alzheimer's disease. J Neurochem 2003;85:115–122.
34. Meiners S, Heyken D, Weller A, et al. Inhibition of proteasome activity induces concerted expression of proteasome genes and de novo formation of mammalian proteasomes. J Biol Chem 2003;278:21517–21525.
35. Choi SH, Joe EH, Kim SU, Jin BK. Thrombin-induced microglial activation produces degeneration of nigral dopaminergic neurons in vivo. J Neurosci 2003;23:5877–5886.
36. Tatton NA. Increased caspase 3 and Bax immunoreactivity accompany nuclear GAPDH translocation and neuronal apoptosis in Parkinson's disease. Exp Neurol 2000;166:29–43.
37. Hashimoto M, Hsu LJ, Sisk A, et al. Human recombinant NACP/alpha-synuclein is aggregated and fibrillated in vitro: relevance for Lewy body disease. Brain Res 1998;799: 301–306.
38. Beal MF. Experimental models of Parkinson's disease. Nat Rev Neurosci 2001;2:325–334.
39. Betarbet R, Sherer TB, MacKenzie G, et al. Chronic systemic pesticide exposure reproduces features of Parkinson's disease. Nat Neurosci 2000;3:1301–1306.
40. Hoglinger GU, Feger J, Prigent A, et al. Chronic systemic complex I inhibition induces a hypokinetic multisystem degeneration in rats. J Neurochem 2003;84:491–502.
41. Lapointe N, St-Hilaire M, Martinoli MG, et al. Rotenone induces non-specific central nervous system and systemic toxicity. FASEB J 2004;18:717–719.

42. Fleming SM, Zhu C, Fernagut P-O, et al. Behavioral and immunohistochemical effects of chronic intravenous an subcutaneous infusions of varying doses of rotenone. Exp Neurol 2004; 187:418–429.
43. Fenteany G, Schreiber SL. Lactacystin, proteasome function, and cell fate. J Biol Chem 1998;273:8545–8548.
44. Sin N, Kim KB, Elofsson M, et al. Total synthesis of the potent proteasome inhibitor epoxomicin: a useful tool for understanding proteasome biology. Bioorg Med Chem Lett 1999;9:2283–2288.
45. Koguchi Y, Kohno J, Nishio M, et al. TMC-95A, B, C, and D, novel proteasome inhibitors produced by Apiospora montagnei Sacc. TC 1093. Taxonomy, production, isolation, and biological activities. J Antibiot (Tokyo) 2000;53:105–109.
46. Nam S, Smith DM, Dou QP. Ester bond-containing tea polyphenols potently inhibit proteasome activity in vitro and in vivo. J Biol Chem 2001;276:13322–13330.
47. Kazi A, Urbizu DA, Kuhn DJ, et al. A natural musaceas plant extract inhibits proteasome activity and induces apoptosis selectively in human tumor and transformed, but not normal and non-transformed, cells. Int J Mol Med 2003;12:879–887.
48. Jana NR, Dikshit P, Goswami A, Nukina N. Inhibition of proteasomal function by curcumin induces apoptosis through mitochondrial pathway. J Biol Chem 2004;279:11680–11685.
49. Ensign JC, Normand P, Burden JP, Yallop CA. Physiology of some actinomycete genera. Res Microbiol 1993;144:657–660.
50. Cross T. Aquatic actinomycetes: a critical survey of the occurrence, growth and role of actinomycetes in aquatic habitats. J Appl Bacteriol 1981;50:397–423.
51. Priyadarshi A, Khuder SA, Schaub EA, Priyadarshi SS. Environmental risk factors and Parkinson's disease: a metaanalysis. Environ Res 2001;86:122–127.